Preparation and Properties of Stearic Acid/Nanocellulose Composite Phase Change Energy Storage Materials

Yufeng ZHAO, Yanghua CHEN *

College of Advanced Manufacturing, Nanchang University, Nanchang 330031, China

http://doi.org/10.5755/j02.ms.36560

Received 7 March 2024; accepted 3 May 2024

To solve the problems of liquid phase leakage and poor thermal conductivity of organic phase change energy storage materials, a novel composite phase change energy storage material (SA/CNF) based on stearic acid (SA) and nanocellulose (CNF) was prepared in this study and added graphene to enhance its thermal conductivity. For the prepared composite phase change materials (SFs) with different ratios, shape stability, and testing experiments showed that the maximum adsorption rate of CNF on SA reached 80 %. The properties of SA/CNF were then characterized by various instruments. The results show that SA and CNF are compounded together by physical interaction. More than 93 % of SA in the composite phase change energy storage material SA/CNF is able to store and release heat through the phase change process, and the latent heat of phase change of pure SA is 206.3 J/g, while the latent heat of phase change of the composite phase change material SA/CNF with 20 % of CNF is 156.2 J/g, and they both have good cycling stability. The addition of graphene enhances the thermal conductivity of SA/CNF to a large extent, and the thermal conductivity at a graphene ratio of 5 % is 261 % higher than that of SA/CNF without graphene. SA/CNF is an environmentally friendly energy storage material with very high application prospects.

Keywords: phase change energy storage materials, thermal conductivity, latent heat, environmentally friendly.

1. INTRODUCTION

Energy plays a vital role in the progress and development of human society and is also an important basis for economic development. However, the situation of energy resources is grim. Oil and coal, as important fossil energy sources, are non-renewable energy sources and will one day be exhausted. Faced with the energy crisis and ecological deterioration, energy transition, namely the development of renewable energy and the development and utilization of new energy sources is extremely urgent [1]. Improving energy utilization and developing new energy sources [2] (e.g., solar energy, wind energy, etc.) have great economic value and important social effects, but the development of new energy sources is susceptible to seasonal variations, geographic differences, and alternation of day and night, which greatly limits their collection and application [3]. Thermal energy storage (TES) using phase change materials [4], which is a kind of energy storage medium, can improve the utilization of energy and thus effectively utilize energy by storing and releasing energy through the thermal effect in the reversible phase change process.

Phase change energy storage materials can be categorized into organic, inorganic, and composite phase change energy storage materials. Organic phase change materials have the advantages of large latent heat of phase change, stable chemical properties, small degree of subcooling, small corrosion, no phase separation, and low cost. Three of the most representative organic solid-liquid phase change materials are SA, paraffin, and polyethylene glycol (PEG). However, they have some drawbacks, mainly low thermal conductivity and material susceptibility to liquid phase leakage [5]. Therefore, improving the thermal conductivity of the materials and solving the problem of liquid-phase leakage are of great importance to promote the application of solid-liquid phase change energy storage materials.

Encapsulation of organic solid-liquid phase change materials using the adsorption effect of porous media is an important way to solve the liquid phase leakage problem. Chen et al. successfully prepared poly(ethylene glycol)/poly(acrylamide)/silica composite phase-change materials [6], and utilized the expanded graphite for the adsorption of n-decanol and lauryl alcohol eutectic materials to prepare a novel composite phase change material [7]. Ma et al. adsorbed erythritol in expanded graphite with high thermal conductivity [8]. Ao prepared a SA/BN novel composite phase change material by melt blending method to improve the thermal conductivity of SA [9]. Nanocellulose (CNF) is an abundant natural organic polymer mainly found in the cell walls of algae and green plants, which has good mechanical properties such as flexibility, elasticity and lightness. Wang et al. modified the surface of nanocellulose with dopamine to achieve up to 95 % encapsulation of PEG, and the latent heat release of PEG was increased by 18.9 %, which effectively promoted the phase change behavior of PEG and improved the thermal

* Corresponding author. Tel.: +86-13970944938.

E-mail: *chenyh@ncu.edu.cn* (Y. Chen)

storage properties of PEG [10]. Shen et al. prepared shape-stabilized composite phase change materials with enhanced thermal conductivity by using nanocellulose-based foams as the support matrix [11]. In addition, some materials play an important role in energy transition, including biomass synthesis, and Mohammad et al. used shape stabilization to improve the mechanical durability of paper, using the right ratio of paraffin waxes to increase paper storage properties [12].

Composite phase change materials prepared from organic solid-liquid phase change materials and organic porous materials generally have the problem of poor thermal conductivity. In recent years, important progress has been made in the utilization of highly thermally conductive nanomaterials composited with phase change energy storage materials, and studies have shown that conventional phase change materials with added nanomaterials have better thermal conductivity compared with the matrix materials [13]. Nanomaterials currently studied for enhanced heat transfer in phase change energy storage materials mainly include nanoparticles [14 – 16], metal foams [17 – 19], carbon nanotubes [20, 21], and graphene [22 – 24]. The n-octadecane/titanium dioxide nanocomposites prepared by Motahar et al. showed that the thermal conductivity enhancement was strongest when the nanoparticles were at a percentage content of 3 % in the solid state [25].

To solve the problems of liquid phase leakage and poor thermal conductivity of organic phase change energy storage materials, the composite phase change material SA/CNF prepared by using lightweight and soft nanocellulose as the backbone, stearic acid as the phase change energy storage material with a phase change temperature of 70 °C, adsorption of SA with CNF, and enhancement of thermal conductivity with graphene was used in this study. Distinguishing from the traditional melt blending method [26] for the preparation of composites, an experimental scheme of mixing and freeze-drying followed by heating and adsorption was designed, taking into account that the phase transition temperature of stearic acid is high and the evaporation of water vapor would cause damage to the surface structure of the skeletal CNF. For the prepared SA/CNF, a field emission ambient scanning electron microscope system (SEM) was used to observe the microscopic morphology, a Fourier transform infrared spectrometer (FTIR) was used to analyze the chemical compatibility of SA and CNF, an X-ray diffractometer (XRD) was used to analyze the physical phase, a differential scanning calorimeter (DSC) was used to determine the phase transition parameters, a thermogravimetric analyzer (TGA) was used to detect its thermal stability, and finally The thermal conductivity of the composite phase change materials (SFCs) with different proportions of graphene was measured. In this study, an environmentally friendly green skeleton was utilized to adsorb hard acids to achieve safety and environmental protection, while two organic materials were composited and thermally enhanced with graphene to develop a new type of composite phase change material with no liquid-phase leakage, good thermal conductivity, and environmentally friendly, which can be applied to structurally complex environments.

2. EXPERIMENTAL SECTION

2.1. Materials and preparation of SA/CNF

Stearic acid ($C_{18}H_{36}O_2$, octadecanoic acid, AR) was purchased from Sinopharm Chemical Reagent Co., Ltd, nanocellulose CNF aqueous dispersion was purchased from Huzhou ScienceK new material Technology Co., Ltd (prepared by oxidation method, containing carboxyl groups), and graphene (multilayered, with 99 % carbon content) was purchased from Shenzhen Suiheng Graphene Co., Ltd.

Table 1. Ratio of the samples

Sample	SA, %	CNF, %	Graphene, %
SF20	80	20	–
SF15	85	15	–
SF10	90	10	–
SF5	95	5	–
SFC0.1	79.9	20	0.1
SFC0.3	79.7	20	0.3
SFC0.5	79.5	20	0.5
SFC1	79	20	1
SFC3	77	20	3
SFC5	75	20	5

Considering the high melting point of SA, this paper proposed a new experimental method. Compared with the traditional melt blending method [27], it can effectively avoid damaging the surface structure of CNF due to water vapor evaporation, as shown in Fig. 1. The proportions between each sample are shown in Table 1.

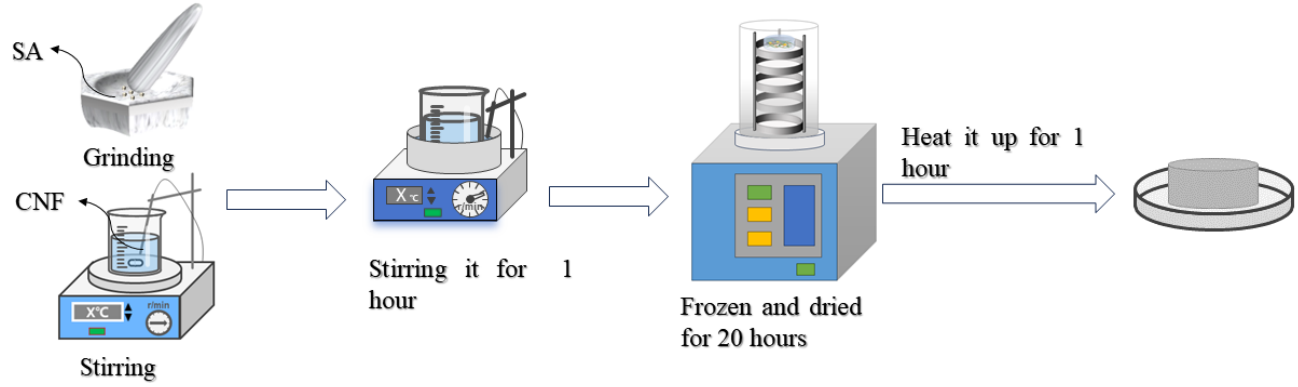

Fig. 1. Preparation process of SA/CNF

Firstly, the granular stearic acid was ground into powder, and at the same time, CNF was magnetically stirred with a collector-type thermostatic heating magnetic stirrer (DF-101Z, China) for 30 minutes to remove the air bubbles inside, and then both of them were stirred for 1 hour at ambient temperature and then poured into molds, and then it was pre-cooled for 3 hours before being put into the vacuum freeze drier (YTLG-10A, China), and then it was put into the upper layer of the freeze drier for 20 hours. Freeze-drying was done for 20 hours. Finally, the freeze-dried samples were put into an electric blast dryer (101-00B, China) and heated at 80 °C for 1 hour. The melted SA would be absorbed by the pores of the CNF, and finally, the prepared samples were obtained. After determining the maximum adsorption rate of CNF on SA, graphene was added to the material for thermal conductivity enhancement of SA/CNF.

2.2. Characterization

The microstructures of CNF, SA/CNF prepared by conventional melt blending method, and SA/CNF prepared by the new experimental method were observed using a field emission ambient scanning electron microscope system (SEM，Quanta 200FEG, America). The infrared spectra of SA, CNF, SF20, and SFC were measured using a Fourier transform infrared spectrometer (FTIR, Nicolet 5700, USA) with a wave number range of 4000 – 400 cm^{-1} and a resolution of 4 cm^{-1}. The chemical structures of SA, CNF, SF20, and SFC were measured using an X-ray diffractometer (XRD, D8 ADVANCE, Germany) with a test angle of 5 – 70 degrees. The thermal properties of SA, SF5, SF10, SF15, and SF20 were measured using differential scanning calorimetry (DSC, DSC 8000, USA) under heating or cooling conditions at a rate of 10 °C/min in a nitrogen atmosphere. Measurements of SA, CNF, SF20, SF15, SF10, SF5, and SFC1 were carried out using a thermogravimetric analyzer (TGA，TGA 4000，America) to check their thermal stability, and the measurement conditions were heating from 25 °C to 700 °C at a rate of 10 °C/min under a nitrogen atmosphere. Finally, the thermal conductivity of SA, SF20, SFC0.1, SF0.3, SFC0.5, SFC1, SFC3, and SFC5 was measured using a thermal conductivity measuring instrument.

3. RESULTS AND DISCUSSION

3.1. Shape stability and leakage testing

Morphological stability and leakage test is mainly examined by the stability of the appearance morphology and phase change material above the phase change temperature, the specific measure is to heat the prepared sample on filter paper in a beaker in a water bath at 80 °C for 30 min, 80 °C is much higher than the melting temperature of SA, the molten SA will be adsorbed by the CNF, if the adsorption of the CNF on the SA reaches saturation, the filter paper after heating will appear traces of SA liquid phase leakage. Specific pictures before and after heating the sample are shown in Fig. 2.

It can be seen from Fig. 2, that when the dry mass ratio of CNF is 5 %, there are serious traces of liquid phase leakage of SA, with the increase of the dry mass ratio of CNF, the traces of liquid phase leakage of SA decrease gradually, and the properties of the composite phase-change material SA/CNF are kept stable, and the shape of SA is kept good without leakage traces when the dry mass ratio of CNF is 20 %, which shows that the adsorption rate of CNF on SA reaches 80 %, and at the same time, an increase in the proportion of the dry mass of the CNF can improve the shape stability of SA/CNF, which proves the feasibility of encapsulating SA with CNF. Based on CNF dry mass share of 20 %, different proportions of graphene were added in the experiments. “xwt.%” represents the ratio of graphene in the composite phase change material SA/CNF, and the samples also remained shape-stable after heating on the filter paper without liquid phase leakage.

Fig. 2. Images of composite phase change material SA/CNF before and after leakage testing

3.2. Morphology and microstructure

The microscopic morphology of the prepared samples is shown in Fig. 3, where Fig. 3 a and Fig. 3 b indicates the microscopic morphology of CNF, and it can be observed that the labeled places have a very large number of pore structures, which can provide a large encapsulation space for SA, and it is a guarantee for realizing a high encapsulation rate for SA. Fig. 3 c and Fig. 3 d show SA/CNF prepared by the conventional melt blending method, and it can be observed that mixing and heating them prior to lyophilization leads to the destruction of nanocellulose surface structure caused by the evaporation of water vapor, which is very unfavorable for the encapsulation of stearic acid.

Fig. 3 e and Fig. 3 f show the SA/CNF prepared by mixing first and then heating method, comparing to the surface structure of nanocellulose in Fig. 3 c and Fig. 3 d, it can be observed that there is no disruption of the surface structure of the nanocellulose, and where the pores were originally shown have been filled with SA, and dispersed SA, indicating that the encapsulation of SA by CNF has reached saturation.

3.3. FTIR analysis

Fig. 4 shows the FT-IR spectra of CNF, SA, SF20 and SFC1. As shown in the figure, the absorption peaks at CNF are represented mainly by the -OH stretching vibration peak at 3347 cm^{-1}, the C=O stretching vibration at 1600 cm^{-1} and the C-O stretching vibration at 1063 cm^{-1}, which is caused

by the fact that CNF is prepared by oxidation and contains carboxyl and hydroxyl groups on its surface, which agrees with that in the literature [28].

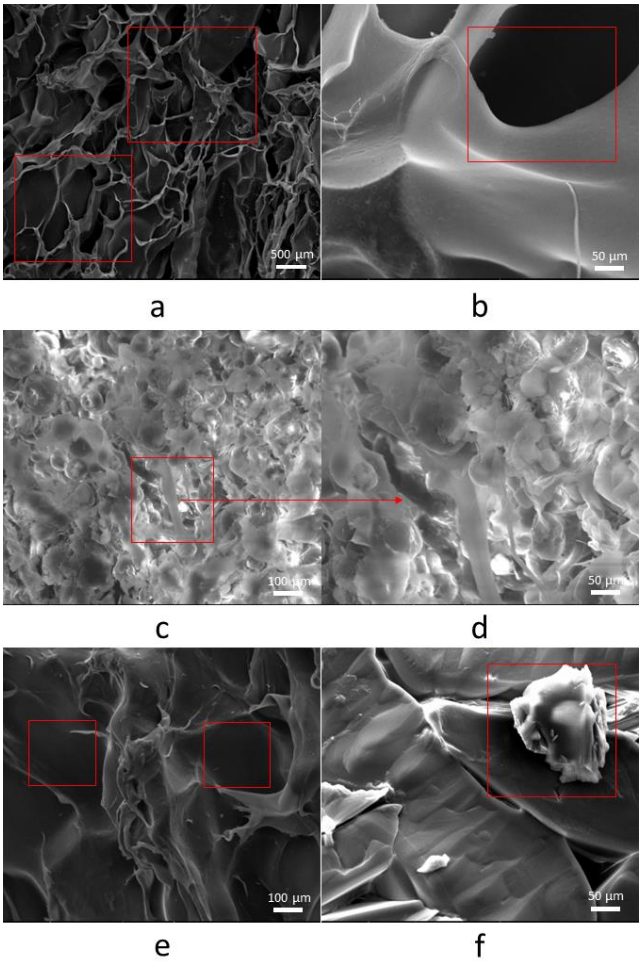

Fig. 3. SEM images: a, b – CNF; c – d-SA/CNF prepared by traditional melt blending method; e – f-SA/CNF prepared by a new experimental method

From the SA profile, it can be seen that the absorption peak at 2957 cm^{-1} is the asymmetric telescopic vibration peak of -CH_3, the absorption peaks at 2914 cm^{-1} and 2850 cm^{-1} are the asymmetric and symmetric telescopic vibration peaks of -CH_2, the absorption peaks with a width of 3000 – 2500 cm^{-1} are the telescopic vibration peaks of -OH, and the absorption peak at 1701 cm^{-1} represents the C=O stretching vibrational peak in carboxylic acids, the absorption peak at 1470 cm^{-1} represents the C-H asymmetric bending vibrational peak in CH_3 groups, the absorption peak at 1299 cm^{-1} represents the in-plane bending vibrational peak of -OH, the absorption peak at 945 cm^{-1} is the out-of-plane deformation vibrational peak of -OH, and the absorption peak at 727 cm^{-1} represents the in-plane deformation when there are more than six CH_2-straight chains rocking vibrational peaks, which is in agreement with those in the literature [29, 30]. From the spectrogram of SF20 in Fig. 4 c. SF20 contains all the characteristic peaks of SA and CNF and there is no appearance of new characteristic peaks, and the surface CNF is simply physiosorbed on SA without the occurrence of chemical reaction, and it can be found that the addition of graphene has no chemical effect on the composite phase change material SA/CNF in the spectrogram of SFC1.

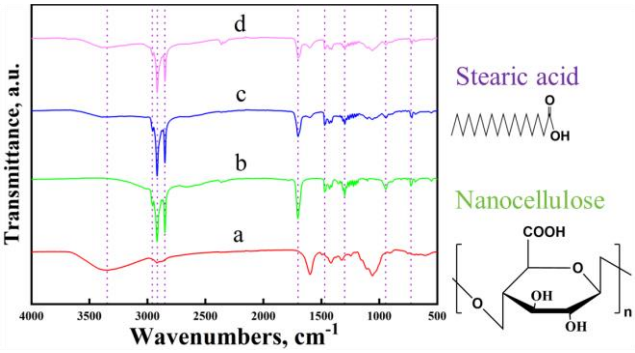

Fig. 4. FTIR spectra: a – CNF; b – SA; c – SF20; d – SFC1

3.4. XRD analysis

Fig. 5 shows the XRD patterns of CNF, SA, SF20 and SFC1. CNF has a characteristic diffraction peak at 2θ = 23.0°, which is broad due to the large amount of amorphous phase in CNF [31]. SA shows four strong typical diffraction peaks at 2θ = 6.7°, 11.1°, 21.6°, and 24.2°, which is consistent with that in the reference [9].

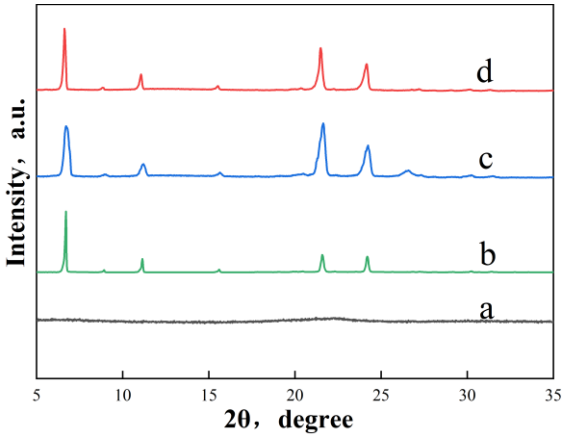

Fig. 5. XRD patterns: a – CNF; b – SA; c – SF20; d – SFC1

From the XRD patterns of SF20 and SFC1, it can be seen that the peaks in the composite phase change material are higher, which indicates that the encapsulated SA is well developed in the crystal in CNF, and the object is higher, and at the same time, the adsorption of SA by CNF has no effect on the position of the characteristic peaks of SA, and the position of the characteristic peaks of the SA/CNF with the addition of graphene has not been changed, and there are no new characteristic peaks in the composite phase change material, so that these two substances are combined by physical form [32]. This means that SA is chemically compatible with CNF.

3.5. Thermal properties analysis

By measuring the enthalpy of melting and enthalpy of solidification of SA/CNF, the encapsulation efficiency of SA in SA/CNF can be calculated as E by Eq. 1 [33] and encapsulation rate R by Eq. 2 [34].

$$E = \frac{\Delta H_{M,comp} + \Delta H_{S,comp}}{\Delta H_{M,PCM} + \Delta H_{S,PCM}} \times 100\%; \quad (1)$$

$$R = \frac{\Delta H_{M,comp}}{\Delta H_{M,PCM}} \times 100\%, \quad (2)$$

where $\Delta H_{M,comp}$ and $\Delta H_{S,comp}$ are the enthalpies of melting and solidification of SA/CNF composites, and $\Delta H_{M,PCM}$ and $\Delta H_{S,PCM}$ are enthalpies of melting and solidification of pure SA. The encapsulation efficiency and encapsulation rate represent the evaluation of the heat storage and exothermic properties of the PCM in the composite phase change material.

Firstly, it can be seen from Fig. 6 a and Fig. 6 b that there are two obvious absorptive and exothermic peaks in the DSC curves about the SA/CNF composite phase change material, which indicates that SA/CNF has good heat storage and exothermic properties, and the absorptive peaks are similar to the exothermic peaks of the prepared composite phase change material SA/CNF, which indicates that the use of CNF as a backbone has not changed the absorptive and exothermic properties of SA.

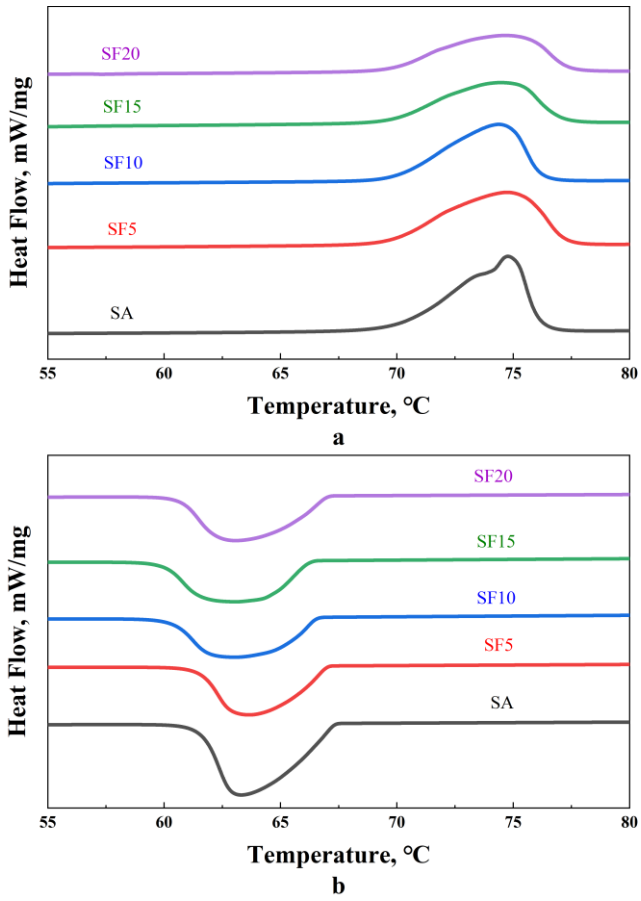

Fig. 6. a – heating DSC curves; b – cooling DSC curves

From the figure, it can be seen that the peak area decreases with the increase of the CNF ratio, which is due to the fact that the support material is inert in the temperature range studied [35], and the addition of CNF does not contribute to the release of latent heat and heat storage, and therefore the enthalpy of melting and solidification decreases.

Then the software integrates the heat absorption and exothermic peaks, and the obtained values of melting temperature, enthalpy of melting, solidification temperature, and enthalpy of solidification are shown in Table 2, where T_M denotes the melting temperature, H_M denotes the latent heat of melting, H_{LM} denotes the theoretical latent heat of melting, T_S denotes the solidification temperature, H_S denotes the latent heat of solidification, and H_{LS} denotes the theoretical latent heat of solidification. The melting temperature of the SA was 71.75 C, the latent heat of melting is 206.3 J/g and the solidification temperature is 67.54 °C with the latent heat of solidification being 204.1 J/g. The melting temperature of the composites is lower than that of pure SA, which is due to the fact that there are weak interactions between the CNF as an adsorbent skeleton and the SA, such as hydrogen bonding, surface tension, etc., and these weak interactions will limit the release of latent heat from the SA and the storage of heat [36], and this leads to the actual SA/ CNF composite phase change materials, the enthalpy of melting and solidification of SA are lower than the theoretical values. Observing the melting and solidification temperatures in Table 2 in conjunction with the curves in Fig. 6. It can be observed that the melting and solidification temperatures of SA and SA/CNF do not coincide with each other, which is attributed to the supercooling behavior of SA.

The data calculated by Eq. 1 and Eq. 2 are shown in Table 3. The encapsulation efficiency E of SF5, SF10, SF15, and SF20 are 91.9 %, 84.7 %, 80.4 %, and 77.4 %, and it can be seen that the encapsulation efficiency corresponding to each sample is lower than the theoretical value, which is due to the fact that the SA crystallizes inside the pore space of the CNF, which acts as melting and solidification of the SA limiting effect. The corresponding encapsulation rates R for each sample are 96 %, 93.2 %, 94.4 %, and 94.7 %, which indicates that more than 93 % of the SA in the SA/CNF of each composite can store and release heat efficiently through the phase transition process.

Table 2. SA/CNF encapsulation efficiency E and encapsulation rate R

Samples	SF5	SF10	SF15	SF20
E, %	91.9	84.7	80.4	77.4
R, %	96.0	93.2	94.4	94.7

Table 3. Thermal performance parameters of the SA/CNF phase transition process

Samples	Heating process			Cooling process		
	T_M, °C	H_M, J/g	H_{LM}, J/g	T_S, °C	H_S, J/g	H_{LS}, J/g
SA	71.75	Δ206.3	–	67.54	Δ204.1	–
SF5	69.84	Δ187.8	Δ195.7	66.98	Δ189.4	Δ193.9
SF10	69.83	Δ173.0	Δ185.7	66.20	Δ174.5	Δ183.7
SF15	70.06	Δ165.5	Δ175.4	66.95	Δ164.5	Δ173.5
SF20	69.93	Δ156.2	Δ165.0	66.50	Δ161.3	Δ163.3

3.6. Thermal conductivity

Thermal conductivity is one of the important parameters for evaluating phase change materials for low-temperature thermal storage applications, but the inherent thermal conductivity of organic phase change energy storage materials is relatively low, in this study, the two organic materials composite substances were thermally enhanced with graphene and measured by using a thermal conductivity measuring instrument. The specific operation steps are to take advantage of CNF has excellent flexibility and mechanical properties, the two prepared SFC extruded into the surface of the same shape of the same samples, the temperature sensor is placed in the middle of the two samples, and then measured three times to take the average value, the specific measurement of the data as shown in Fig. 7.

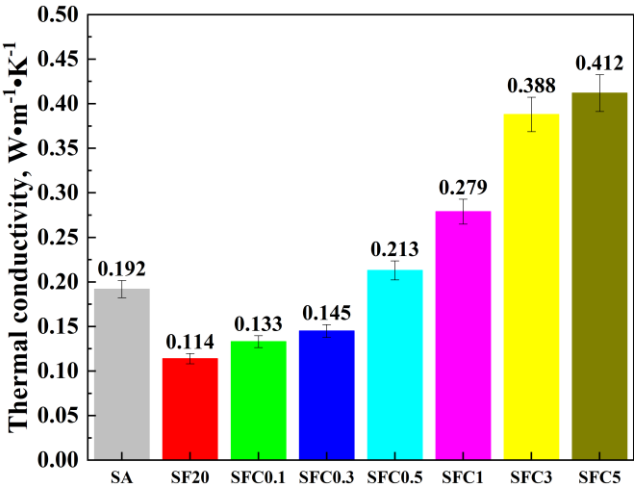

Fig. 7. Thermal conductivity of SA/CNF with graphene addition

From Fig. 7, it can be seen that the thermal conductivity of pure SA is higher than that of the prepared SA/CNF, which is due to the fact that CNF belongs to the organic material while possessing a large porosity, which enters into the air and restricts the thermal conductivity of SA. As the proportion of graphene increases, the thermal conductivity of the composite phase change energy storage material gradually increases, and the thermal conductivity exceeds that of pure SA when the proportion of graphene is 0.5 %. When the proportion of graphene reaches 5%, the thermal conductivity of SFC5 is 0.412 $W \cdot m^{-1} \cdot K^{-1}$, which is 114 % higher than that of pure SA , which is 261 % higher than the thermal conductivity of the composite phase change material SF20 without graphene addition. From the figure, it can be found that the thermal conductivity improved by increasing the proportion of graphene from 3 % to 5 % in the composite phase change energy storage material is much smaller than that improved by increasing it from 1 % to 3 %, which is because excessive graphene leads to unwanted aggregation, which serves as a barrier to thermal conductivity. Also, an increase in the proportion of graphene leads to a decrease in the proportion of SA, which reduces the latent heat of phase transition of the composite phase change material, so it is important to add the right proportion of nanomaterials.

3.7. Thermal stability

To study the thermal stability of the composite phase change material SA/CNF, SA/CNF was thermogravimetrically analyzed, and the results are shown in Fig. 8.

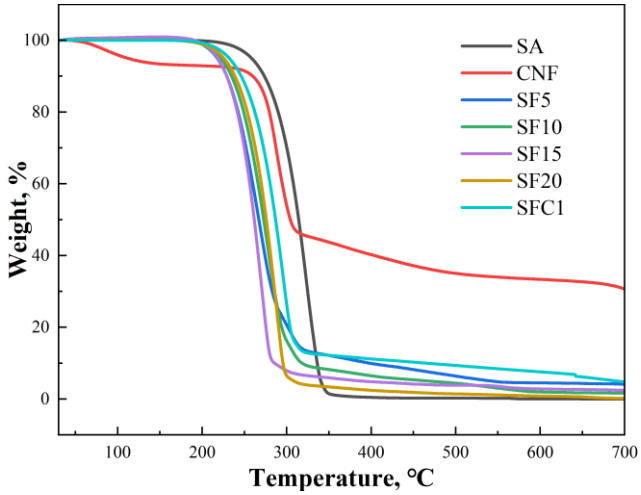

Fig. 8. TGA curves for SA, CNF and SA/CNF

The temperature at which the weight loss of SA starts when heated is 205 °C, and the weight change is small after 360 °C, and it is completely thermally decomposed (98.95 %). There are two thermal decomposition processes of CNF at 42 ~ 105 °C and 220 ~ 700 °C, which is due to the mass reduction in the first part is the part of water adsorbed on CNF, and the second part is the decomposition part of CNF. From the figure, it can be found that the thermal decomposition curves of the composite phase change material SA/CNF are very similar to those of SA, indicating that the addition of CNF did not change the thermal stability characteristics of SA. The temperature at which the decomposition of the composite phase change material SA/CNF starts is lower than that of SA, which is because the CNF starts to decompose first in SA/CNF because the dry mass of CNF accounts for a smaller proportion, and the decomposition of the first part is smaller, and both start to decompose together at 220 ℃. The prepared composite phase change materials should be designed to operate at temperatures below 100 °C. For the prepared samples SF5, SF10, SF15, SF20, and SFC1 the weight loss data were 0.003 %, 0.033 %, 0.037 %, 0.131 %, and 0.203 % at 30 to 100 °C. All the composite phase change materials SA/CNF were able to lose less than 0.203 % of mass within the working temperature, which proves the acceptable thermal stability of SA/CNF.

4. CONCLUSIONS

In this study, a novel composite material SA/CNF with good stability and environmental friendliness was prepared by innovatively using CNF as a skeleton and embedding SA as a phase change material into CNF. The adsorption rate of CNF on SA is as high as 80%, and there is good chemical compatibility between CNF and SA; The composite phase change material SA/CNF has high heat storage and exothermic capacity, the latent heat of phase change of SF20 is 156.2 J/g; SA/CNF has good thermal stability ability, the

weight loss ratio is less than 0.203 % at 30 ~ 100 ℃ working temperature; with the addition of graphene at a ratio of 5 %, the thermal conductivity of SFC5 is 114 % higher than that of pure SA, and 261 % higher than that of SF20, a composite phase change material with no graphene added.

The present study is an attempt to prepare a new composite phase change material based on SA. The prepared SA/CNF has excellent physical properties of flexibility, good mechanical properties, and high latent heat of phase change, and its health and environmental advantages have high application prospects. CNF is a healthy and environmentally friendly green material, and the composite phase change material SA/CNF with CNF as the substrate is expected to be applied to the thermal management of human body, but the problem of human body's adaptability to the composite phase change material SA/CNF has not been solved yet; Although the CNF-based composite phase change material SA/CNF has high flexibility and mechanical strength, it is still difficult to be applied to high-strength scenarios, and its mechanical strength needs to be further improved.

Acknowledgments

This work was financially supported by the Innovation Foundation for Postgraduate of Jiangxi (YC2022-s023).

REFERENCES

1. **Gao, H., Wang, J., Chen, X., Wang, G., Huang, X., Li, A., Dong, W.** Nanoconfinement Effects on Thermal Properties of Nanoporous Shape-stabilized Composite PCMs: A Review *Nano Energy* 53 2018: pp. 769 – 797. http://doi.org/10.1016/j.nanoen.2018.09.007
2. **Muzhanje, A.T., Hassan, M.A., Ookawara, S., Hassan, H.** An Overview of the Preparation and Characteristics of Phase Change Materials with Nanomaterials *Journal of Energy Storage* 51 2022: pp. 104353. http://doi.org/10.1016/j.est.2022.104353
3. **Jouhara, H., Żabnieńska-Góra, A., Khordehgah, N., Ahmad, D., Lipinski, T.** Latent Thermal Energy Storage Technologies and Applications: A Review *International Journal of Thermofluids* 5 – 6 2020: pp. 100039. http://doi.org/10.1016/j.ijft.2020.100039
4. **Fallahi, A., Guldentops, G., Tao, M., Granados-Focil, S., Van Dessel, S.** Review on Solid-Solid Phase Change Materials for Thermal Energy Storage: Molecular Structure and Thermal Properties *Applied Thermal Engineering* 127 2017: pp. 1427 – 1441. http://doi.org/10.1016/j.applthermaleng.2017.08.161
5. **Chinnasamy, V., Heo, J., Jung, S., Lee, H., Cho, H.** Shape Stabilized Phase Change Materials Based on Different Support Structures for Thermal Energy Storage Applications – A Review *Energy* 262 2023: pp. 125463. http://doi.org/10.1016/j.energy.2022.125463
6. **Chen, Y., Pei, Y., Yang, X.** Synthesis and Performance Analysis of a Novel Phase Change Hydrogel Polyethylene Glycol/Polyacrylamide/Silicon Dioxide for Thermal Energy Storage *Materials Science (Medžiagotyra)* 29 (3) 2023: pp. 316 – 322. http://doi.org/10.5755/j02.ms.32914
7. **Liu, Y., Chen, Y.** Preparation and Properties of Lauryl Alcohol-Caprylic Acid Eutectics/Activated Charcoal Composites as Shape-stabilized Phase Change Materials for Cold Energy Storage *Materials Science (Medžiagotyra)* 26 (3) 2020: pp. 300 – 307. http://doi.org/10.5755/j01.ms.26.3.21371
8. **Ma, C., Wang, J., Wu, Y., Wang, Y., Ji, Z., Xie, S.** Characterization and Thermophysical Properties of Erythritol/Expanded Graphite as Phase Change Material for Thermal Energy Storage *Journal of Energy Storage* 46 2022: pp. 103864. http://doi.org/10.1016/j.est.2021.103864
9. **Ao, C., Yan, S., Zhao, X., Zhang, N., Wu, Y.** Stearic Acid/Boron Nitride as a Composite Phase Change Material For Thermal Energy Storage *Diamond and Related Materials* 133 2023: pp. 109671. http://doi.org/10.1016/j.diamond.2022.109671
10. **Wang, H., Deng, Y., Wu, F., Jin, H., Liu, Y., Zheng, J.** Facile In-Situ Fabrication of Latent Heat Enhanced Cellulose Aerogel-Based Form-Stable Composite Phase Change Materials Based on Dopamine Modification Strategy *Solar Energy Materials and Solar Cells* 230 2021: pp. 111236. http://doi.org/10.1016/j.solmat.2021.111236
11. **Shen, Z., Kwon, S., Lee, H.L., Toivakka, M., Oh, K.** Preparation and Application of Composite Phase Change Materials Stabilized by Cellulose Nanofibril-Based Foams for Thermal Energy Storage *International Journal of Biological Macromolecules* 222 (Pt B) 2022: pp. 3001 – 3013. http://doi.org/10.1016/j.ijbiomac.2022.10.075
12. **Mohammad Firman, L.O., Adji, R.B., Ismail Rahman, R.A.** Increasing the feasibility and Storage Property of Cellulose-Based Biomass by Forming Shape-Stabilized Briquette with Hydrophobic Compound *Case Studies in Chemical and Environmental Engineering* 8 2023: pp. 100443. http://doi.org/10.1016/j.cscee.2023.100443
13. **Mettawee, E.B. S., Assassa, G.M.R.** Thermal Conductivity Enhancement in a Latent Heat Storage System *Solar Energy* 81 (7) 2007: pp. 839 – 845. http://doi.org/10.1016/j.solener.2006.11.009
14. **Masoumi, H., Haghighi Khoshkhoo, R., Mirfendereski, S.M.** Experimental and Numerical Investigation of Melting/Solidification of Nano-Enhanced Phase Change Materials in Shell & Tube Thermal Energy Storage Systems *Journal of Energy Storage* 47 2022: pp. 103561. http://doi.org/10.1016/j.est.2021.103561
15. **Colla, L., Fedele, L., Mancin, S., Danza, L., Manca, O.** Nano-PCMs for Enhanced Energy Storage and Passive Cooling Applications *Applied Thermal Engineering* 110 2017: pp. 584 – 589. http://doi.org/10.1016/j.applthermaleng.2016.03.161
16. **Sheikh, Y., Orhan, M.F., Umair, M., Mehaisi, E., Azmeer, A.** Variation in Cooling Performance of a Bio-Based Phase Change Material by Adding Graphene Nanoplatelets with Surfactants *International Journal of Thermofluids* 16 2022: pp. 100201. http://doi.org/10.1016/j.ijft.2022.100201
17. **Xu, Y., Li, M.J., Zheng, Z.J., Xue, X.D.** Melting Performance Enhancement of Phase Change Material by a Limited Amount of Metal Foam: Configurational Optimization and Economic Assessment *Applied Energy* 212 2018: pp. 868 – 880. http://doi.org/10.1016/j.apenergy.2017.12.082
18. **Zhu, Z.Q., Huang, Y.K., Hu, N., Zeng, Y., Fan, L.W.** Transient Performance of a PCM-Based Heat Sink with a Partially Filled Metal Foam: Effects of the Filling Height Ratio *Applied Thermal Engineering* 128 2018: pp. 966 – 972.

http://doi.org/10.1016/j.applthermaleng.2017.09.047

19. **Jin, H.Q., Fan, L.W., Liu, M.J., Zhu, Z.Q., Yu, Z.T.** A pore-Scale Visualized Study of Melting Heat Transfer of a Paraffin Wax Saturated in a Copper Foam: Effects of the Pore Size *International Journal of Heat and Mass Transfer* 112 2017: pp. 39 – 44. http://doi.org/10.1016/j.ijheatmasstransfer.2017.04.114
20. **Yu, Z., Feng, D., Feng, Y., Zhang, X.** Thermal Conductivity and Energy Storage Capacity Enhancement and Bottleneck of Shape-Stabilized Phase Change Composites with Graphene Foam and Carbon Nanotubes *Composites Part A: Applied Science and Manufacturing* 152 2022: pp. 106703. http://doi.org/10.1016/j.compositesa.2021.106703
21. **Anusak, N., Virtanen, J., Kangas, V., Promarak, V., Yotprayoonsak, P.** Enhanced Joule Heating Performance of Flexible Transparent Conductive Double-Walled Carbon Nanotube Films on Sparked Ag Nanoparticles *Thin Solid Films* 750 2022: pp. 139201. http://doi.org/10.1016/j.tsf.2022.139201
22. **Liu, X., Rao, Z.** Experimental Study on the Thermal Performance of Graphene and Exfoliated Graphite Sheet for Thermal Energy Storage Phase Change Material *Thermochimica Acta* 647 2017: pp. 15 – 21. http://doi.org/10.1016/j.tca.2016.11.010
23. **Feng, J., Liu, Z.J., Zhang, D.Q., He, Z., Tao, Z.C.,Guo, Q.G.** Phase Change Materials Coated With Modified Graphene-oxide as Fillers For Silicone Rubber Used in Thermal Interface Applications *New Carbon Materials* 34 (2) 2019: pp. 188 – 195. http://doi.org/10.1016/s1872-5805(19)60011-9
24. **Hasbi, S., Norazman, N., Saharudin, M.S.** Effects of Titanium Oxide and Graphene as Nano-Fillers on the Thermal Conductivity of Biobased Phase Change Materials as Latent Thermal Heat Storage *Materials Today: Proceedings* 75 2023:pp. 181 – 187. http://doi.org/10.1016/j.matpr.2022.11.426
25. **Motahar, S., Nikkam, N., Alemrajabi, A.A., Khodabandeh, R., Toprak, M.S., Muhammed, M.** Experimental Investigation on Thermal and Rheological Properties of N-Octadecane with Dispersed TiO_2 Nanoparticles *International Communications in Heat and Mass Transfer* 59 2014: pp. 68 – 74. http://doi.org/10.1016/j.icheatmasstransfer.2014.10.016
26. **Chen, X., Wang, W., Li, S., Qian, Y., Jiao, C.** Synthesis of TPU/TiO_2 Nanocomposites by Molten Blending Method *Journal of Thermal Analysis and Calorimetry* 132 (1) 2018: pp. 793 – 803. http://doi.org/10.1007/s10973-017-6944-6
27. **Chen, Y., Wang, T., Pei, Y.** Cellulose Nanofiber/Polyethylene Glycol Composite Phase Change Thermal Storage Gel Based on Solid-gel Phase Change *Materials Science (Medžiagotyra)* 30 (2) 2023: pp. 226 – 232. http://doi.org/10.5755/j02.ms.35249
28. **He, Y., Yang, J., Chen, W., Chen, W., Zhao, L., Qi, W.** Gallium-doped MXene/cellulose Nanofiber Composite Membranes with Electro/Photo Thermal Conversion Property for High Performance Electromagnetic Interference Shielding *Chemical Engineering Journal* 464 2023: pp. 142565. http://doi.org/10.1016/j.cej.2023.142565
29. **Li, C., Xie, B., Chen, D., Chen, J., Li, W., Chen, Z., Gibb, S.W., Long, Y.** Ultrathin Graphite Sheets Stabilized Stearic Acid as a Composite Phase Change Material for Thermal Energy Storage *Energy* 166 2019: pp. 246 – 255. http://doi.org/10.1016/j.energy.2018.10.082
30. **Luo, K., Wu, D., Wang, Y., Fei, H., Jiang, H., Ye, Z.** Preparation and Characterization of Lauric Acid-Stearic Acid/Fumed Silica/Expanded Graphite Thermally Conductive Enhanced Composites *Journal of Energy Storage* 73 2023: pp. 109151. http://doi.org/10.1016/j.est.2023.109151
31. **Lin, W.H., Jana, S.C.** Analysis of Porous Structures of Cellulose Aerogel Monoliths and Microparticles *Microporous and Mesoporous Materials* 310 2021: pp. 110625. http://doi.org/10.1016/j.micromeso.2020.110625
32. **Suyitno, B.M., Pane, E.A., Rahmalina, D., Rahman, R.A.** Improving the Operation and Thermal Response of Multiphase Coexistence Latent Storage System Using Stabilized Organic Phase Change Material *Results in Engineering* 18 2023: pp. 101210. http://doi.org/10.1016/j.rineng.2023.101210
33. **Voronin, D.V., Mendgaziev, R.I., Rubtsova, M.I., Cherednichenko, K.A., Demina, P.A., Abramova, A.M., Shchukin, D.G., Vinokurov, V.** Facile Synthesis of Shape-Stable Phase-Change Composites Via the Adsorption of Stearic Acid onto Cellulose Microfibers *Materials Chemistry Frontiers* 6 (8) 2022: pp. 1033 – 1045. http://doi.org/10.1039/d1qm01631h
34. **Yu, S., Wang, X., Wu, D.** Microencapsulation of N-Octadecane Phase Change Material With Calcium Carbonate Shell for Enhancement of Thermal Conductivity and Serving Durability: Synthesis, Microstructure, and Performance Evaluation *Applied Energy* 114 2014: pp. 632 – 643. http://doi.org/10.1016/j.apenergy.2013.10.029
35. **Wang, C., Wang, W., Xin, G., Li, G., Zheng, J., Tian, W., Li, X.** Phase Change Behaviors of PEG on Modified Graphene Oxide Mediated by Surface Functional Groups *European Polymer Journal* 74 2016: pp. 43 – 50. http://doi.org/10.1016/j.eurpolymj.2015.10.027
36. **Zhang, M., Cheng, H., Wang, C., Zhou, Y.** Kaolinite Nanotube-Stearic Acid Composite as a Form-Stable Phase Change Material for Thermal Energy Storage *Applied Clay Science* 201 2021: pp. 105930. http://doi.org/10.1016/j.clay.2020.105930